SuperEncoder: Towards Iteration-Free Approximate Quantum State Preparation

Anonymous Author(s)
Affiliation
Address
email

Abstract

Numerous quantum algorithms operate under the assumption that classical data has already been converted into quantum states, a process termed Quantum State Preparation (QSP). However, achieving precise QSP requires a circuit depth that scales exponentially with the number of qubits, making it a substantial obstacle in harnessing quantum advantage. Recent research suggests using a Parameterized Quantum Circuit (PQC) to approximate a target state, offering a more scalable solution with reduced circuit depth compared to precise QSP. Despite this, the need for iterative updates of circuit parameters results in a lengthy runtime, limiting its practical application. To overcome this challenge, we introduce SuperEncoder, a pre-trained classical neural network model designed to directly estimate the parameters of a PQC for any given quantum state. By eliminating the need for iterative parameter tuning, SuperEncoder represents a pioneering step towards iteration-free approximate QSP.

1 Introduction

Quantum Computing (QC) leverages quantum mechanics principles to address classically intractable problems [47, 36]. Various quantum algorithms have been developed, encompassing quantum-enhanced linear algebra [15, 48, 45], Quantum Machine Learning (QML) [26, 19, 1, 33, 50, 3], quantum-enhanced partial differential equation solvers [31, 13], etc. A notable caveat is that those algorithms assume that classical data has been efficiently loaded into a specific quantum state, a process known as Quantum State Preparation (QSP).

However, the realization of QSP presents significant challenges. Ideally, we expect each element of the classical data to be precisely transformed into an amplitude of the corresponding quantum state. This precise QSP is also known as Amplitude Encoding (AE). However, a critical yet unresolved problem of AE is that the required circuit depth grows exponentially with respect to the number of qubits [34, 41, 29, 46, 49]. Extensive efforts have been made to alleviate this issue, but they fail to address it fundamentally. For example, while some methods introduce ancillary qubits for shallower circuit [57, 56, 2], they may encounter an exponential number of ancillary qubits. Other methods aim at preparing *special* quantum states with lower circuit depth, being only effective for either sparse states [12, 32] or states with some special distributions [14, 17]. To summarize, realizing AE for *arbitrary* quantum states still remains *non-scalable* due to its exponential resource requirement with respect to the number of qubits. Moreover, in the Noisy Intermediate-Scale Quantum (NISQ) era [42], hardware has limited qubit lifetimes and confronts a high risk of decoherence errors when executing deep circuits, further exacerbating the problem of AE.

In fact, precise QSP is unrealistic in the present NISQ era due to the inherent errors of quantum devices. Hence, iteration-based Approximate Amplitude Encoding (AAE) emerges as a promising technique [59, 35, 52]. Specifically, AAE constructs a quantum circuit with tunable parameters, then

Submitted to 38th Conference on Neural Information Processing Systems (NeurIPS 2024). Do not distribute.

it iteratively updates the parameters to approximate a target quantum state. Since the updating of parameters can be guided by states obtained from noisy devices, AAE is robust to noises, becoming especially suitable for NISQ applications. More importantly, AAE has been shown to have shallow circuit depth [35, 52], making it more scalable than AE.

Unfortunately, AAE possesses a drawback that significantly undermines its potential advantages — the lengthy runtime stemming from iterative optimizations of parameters. For example, when a Quantum Neural Network (QNN) [3] is trained and deployed, the runtime of AAE dominates the inference time as we demonstrated in Fig. 1. Since loading classical data into quantum states becomes the bottleneck, the potential advantage of QNN diminishes no matter how efficient the computations are done on quantum devices.

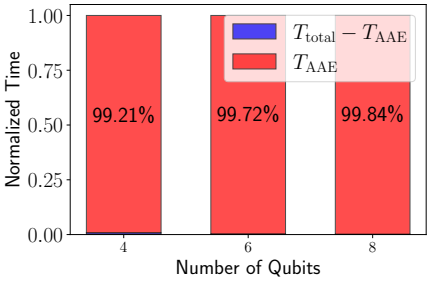

Figure 1: Breakdown of normalized runtime for QNN inference. Original data are listed in Table 1.

Compared to AAE, AE employs a pre-defined arithmetic decomposition procedure to construct a circuit, thereby becoming much *faster* than AAE at runtime. Therefore, it is natural to ask: can we realize both *fast* and *scalable* methods for *arbitrary* QSP? This is precisely the question we tackle in this paper. Overall, we present three major contributions.

- Given a Parameterized Quantum Circuit (PQC) $U(\boldsymbol{\theta})$ that approximates a target quantum state, with $\boldsymbol{\theta}$ the parameter vector. We show that there exists a *deterministic* transformation f that could map an arbitrary state $|\boldsymbol{d}\rangle$ to its corresponding parameters $\boldsymbol{\theta}$. Consequently, the parameters can be designated by f without time-intensive iterations.
- We show that the mapping f is *learnable* by utilizing a classical neural network model, which we term as SuperEncoder. With SuperEncoder, you can have your cake and eat it too, i.e., simultaneously realizing *fast* and *scalable* QSP. We develop a prototype model and shed light on insights into its training methodology.
- We verify the effectiveness of SuperEncoder on both synthetic dataset and representative downstream tasks, paving the way toward iteration-free approximate quantum state preparation.

2 Preliminaries

In this section, we commence with some basic concepts about quantum computing [36], and then proceed to a brief retrospect of existing QSP methods.

2.1 Quantum Computation

We use Dirac notation throughout this paper. A *pure quantum state* is defined by a vector $|\cdot\rangle$ named 'ket', with the unit length. A state can be written as $|\psi\rangle = \sum_{j=1}^{N} \alpha_j |j\rangle$ with $\sum_j |\alpha_j|^2 = 1$, where $|j\rangle$ denotes a computational basis state and N represents the dimension of the complex vector space. *Density operators* describe more general quantum states. Given a mixture of m pure states $\{|\psi_i\rangle\}_{i=1}^{m}$ with probabilities p_i and $\sum_i^m p_i = 1$, the density operator ρ denotes the *mixed state* as $\rho = \sum_{i=1}^{m} p_i |\psi_i\rangle\langle\psi_i|$ with $\mathrm{Tr}(\rho) = 1$, where $\langle\cdot|$ refers to the conjugate transpose of $|\cdot\rangle$. Generally, we use the term *fidelity* to describe the similarity between an erroneous quantum state and its corresponding correct state.

The fundamental unit of quantum computation is the quantum bit, or *qubit*. A qubit's state can be expressed as $\psi = \alpha|0\rangle + \beta|1\rangle$. Given n qubits, the state is generalized to $|\psi\rangle = \sum_j^{2^n} |j\rangle$, where $|j\rangle = |j_1 j_2 \cdots j_n\rangle$ with j_k the state of kth qubit in computational basis, and $j = \sum_{k=1}^{n} 2^{n-k} j_k$. Applying *quantum operations* evolves a system from one state to another. Generally, these operations can be categorized into quantum gates and measurements. Typical single-qubit gates include the Pauli gates $X \equiv \left[\begin{smallmatrix} 0 & 1 \\ 1 & 0 \end{smallmatrix}\right]$, $Y \equiv \left[\begin{smallmatrix} 0 & -i \\ i & 0 \end{smallmatrix}\right]$, $Z \equiv \left[\begin{smallmatrix} 1 & 0 \\ 0 & -1 \end{smallmatrix}\right]$. These gates have associated rotation operations $R_P(\theta) \equiv \mathrm{e}^{-i\theta P/2}$, where θ is the rotation angle and $P \in \{X, Y, Z\}$[1]. Muti-qubit operations create

[1] In this paper, R_z, R_y are equivalent to R_Z, R_Y.

entanglement between qubits, allowing one qubit to interfere with others. In this work, we focus on the controlled-NOT (CNOT) gate, with the mathematical form of $\text{CNOT} \equiv |0\rangle\langle 0| \otimes \mathbf{I}_2 + |1\rangle\langle 1| \otimes X$. Quantum measurements extract classical information from quantum states, which is described by a collection $\{M_m\}$ with $\sum_m M_m^\dagger M_m = \mathbf{I}$. Here, m refers to the measurement outcomes that may occur in the experiment, with a probability of $p(m) = \langle\psi|M_m^\dagger M_m|\psi\rangle$. The post-measurement state of the system becomes $M_m|\psi\rangle/p(m)$.

A *quantum circuit* is the graphical representation of a series of quantum operations, which can be mathematically represented by a unitary matrix U. In the NISQ era, PQC plays an important role as it underpins variational quantum algorithms [11, 39]. Typical PQC has the form of $U(\boldsymbol{\theta}) = \prod_i U_i(\theta_i)V_i$, where $\boldsymbol{\theta}$ is its parameter vector, $U_i(\theta_i) = \mathrm{e}^{-i\theta_i P_i/2}$ with P_i denoting a Pauli gate, and V_i denotes a fixed gate such as CNOT. For example, a PQC composed of R_y gates and CNOT gates is depicted in Fig. 2.

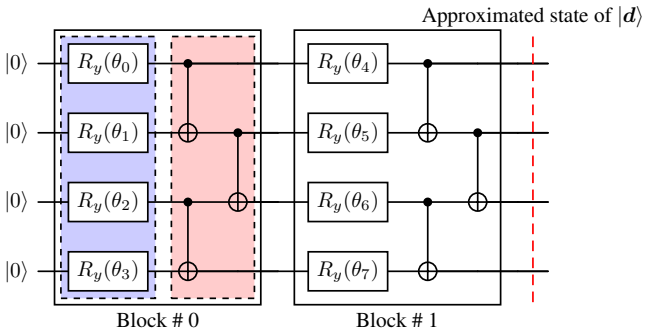

Figure 2: An example PQC with two blocks, with each block consisting of a rotation layer (filled blue) plus an entangler layer (filled red).

2.2 Quantum State Preparation

Successful execution of many quantum algorithms requires an initial step of loading classical data into a quantum state [5, 15], a process known as *quantum state preparation*. This procedure involves implementing a quantum circuit to evolve a system to a designated state. Here, we focus on *amplitude encoding* and formalize its procedure as follows. Let $\boldsymbol{d}$ be a real-valued N-dimensional classical vector, AE encodes $\boldsymbol{d}$ into the amplitudes of an n-qubit quantum state $|\boldsymbol{d}\rangle$, where $N = 2^n$. More specifically, the data quantum state is represented by $|\boldsymbol{d}\rangle = \sum_{j=0}^{N-1} d_j|j\rangle$, where d_j denotes the jth element of the vector $\boldsymbol{d}$, and $|j\rangle$ refers to a computational basis state. The main objective is to generate a quantum circuit U that initializes an n-qubit system by $U|0\rangle^{\otimes n} = \sum_{j=0}^{N-1} \alpha_j|j\rangle$, whose amplitudes $\{\alpha_j\}$ are equal to $\{d_j\}$. It is widely recognized that constructing such a circuit generally necessitates a circuit depth that scales exponentially with n [34, 41]. This property makes AE impractical in current NISQ era, as decoherence errors [23] can severely dampen the effectiveness of AE as the number of qubits increases [52].

In response to the inherent noisy nature of current devices, *approximate amplitude encoding* has emerged as a promising technique [59, 35, 52]. Specifically, AAE utilizes a PQC (a.k.a. ansatz) to approximate the target quantum state by iteratively updating the parameters of circuit, following a similar procedure of other variational quantum algorithms [39, 11]. AAE has been shown to be more advantageous for NISQ devices due to its ability to mitigate coherent errors through flexible adjustment of circuit parameters, coupled with its lower circuit depth [52]. We denote an ansatz as $U(\boldsymbol{\theta})$, where $\boldsymbol{\theta}$ refers to a vector of tunable parameters for optimizations. A typical ansatz consists of several blocks of operations with the same structure. For example, a two-block ansatz with 4 qubits is shown in Fig. 2, where the rotation layer is composed of single-qubit rotational gates $R_y(\theta_r) = \mathrm{e}^{-i\theta_r Y/2}$, and the entangler layer comprises CNOT gates. Note that the entangler layer is configurable and hardware-native, which means that we can apply CNOT gates to physically adjacent qubits, thereby eliminating the necessity of additional SWAP gates to overcome the topological constraints [27]. This type of PQC is also known as *hardware-efficient ansatz* [20], being widely adopted in previous studies of AAE [59, 35, 52].

3 SuperEncoder

3.1 Motivation

Although AAE can potentially realize high fidelity QSP with $O(\text{poly}(n))$ circuit depth [35] with n the number of qubits, it requires repetitive *online* tuning of parameters to approximate the target state, which may result in an excessively long runtime that undermines its feasibility. Specifically, we could consider a simple application scenario in QML. The workflow with AAE is depicted in Fig. 3a. During the inference stage, we must iteratively update the parameters of the AAE ansatz for each input classical data vector, which may greatly dampen the performance. To quantify this impact, we measure the runtime of AAE-based data loading and the total runtime of model inference. As one can observe from Table 1, AAE dominates the runtime, thereby becoming the performance bottleneck.

n	T_{AAE} (s)	$T_{\text{total}} - T_{\text{AAE}}$ (s)
4	**5.0086**	0.0397
6	**20.1810**	0.0573
8	**59.4193**	0.0978

Table 1: **Performance overhead of AAE**. We break down the averaged inference runtime per sample from the MNIST dataset. T_{AAE} denotes time spent on loading classical data into quantum state using AAE, and T_{total} refers to total runtime.

The necessity of time-intensive iterations is grounded in the following assumption — Given an arbitrary quantum state $|\psi\rangle$, there *does not* exist a deterministic transformation $f : |\psi\rangle \to \boldsymbol{\theta}$, where $\boldsymbol{\theta}$ refers to the vector of parameters enabling a PQC to prepare an approximated state of $|\psi\rangle$. This assumption seems intuitively correct given the randomness of target states. However, we argue that a universal mapping f exists for any arbitrary data state $|\psi\rangle$. Taking a little thought of AE, we see that it implies the following conclusion: given an arbitrary state $|\psi\rangle$, there exists an universal arithmetic decomposition procedure $g : |\psi\rangle \to U$ satisfying $U|0\rangle = |\psi\rangle$. Inspired by this deterministic transformation, it is natural to ask: is there an universal transformation $g' : |\psi\rangle \to U'$ satisfying $E(U'|0\rangle, |\psi\rangle) \leq \epsilon$? Here E denotes the deviation between the prepared state by a circuit U' and the target state, and ϵ refers to certain acceptable error threshold. Since the structure of PQC in AAE is the same for any target state, U' is determined by $\boldsymbol{\theta}$. Then, the problem is reduced to exploring the existence of $f : |\psi\rangle \to \boldsymbol{\theta}$. Should f exist, the overhead of online iterations could be eliminated, resulting in a novel QSP method being both fast and scalable.

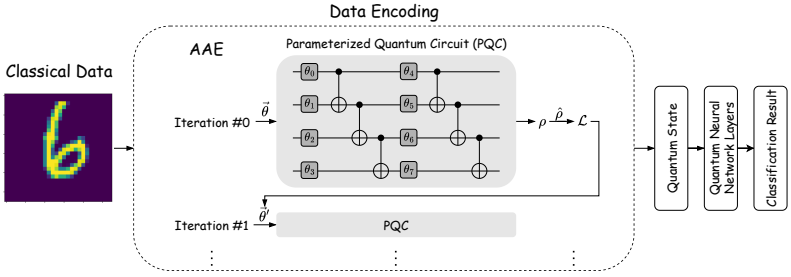

(a) Inference process of AAE.

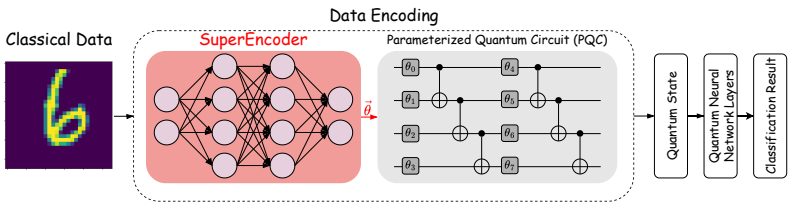

(b) Inference process of SuperEncoder.

Figure 3: Comparison between AAE and SuperEncoder.

3.2 Design Methodology

Let $|\psi\rangle$ be the target state, and $U(\boldsymbol{\theta})$ be the PQC used in AAE with $\boldsymbol{\theta}$ the optimized parameters. Our goal is to develop a model, termed SuperEncoder, to approximate the mapping $f : |\psi\rangle \rightarrow \boldsymbol{\theta}$. Referring back to the scenario in QML, the workflow with SuperEncoder becomes iteration-free, as depicted in Fig. 3b.

Since neural networks could be used to approximate any continuous function [6], a natural solution is to use a neural network to approximate f. Specifically, we adopt a Multi-Layer Perceptron (MLP) as the backbone model for approximating f. However, training this model is nontrivial. Particularly, we find it challenging to design a proper loss function. In the remainder of this section, we explore three different designs and analyze their performance.

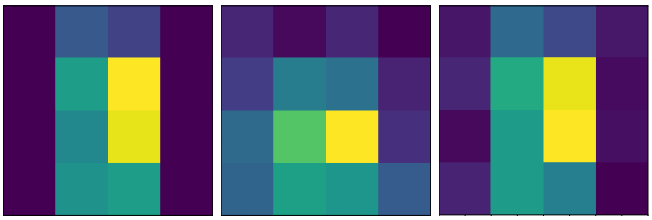

(a) Target state. (b) SuperEncoder-$\mathcal{L}_1$ (c) SuperEncoder-$\mathcal{L}_3$

Figure 4: Virtualization of states generated by SuperEncoder trained with different loss functions. $\mathcal{L}_2$ is omitted as it produces very similar results to $\mathcal{L}_3$.

The first and most straightforward method is *parameter-oriented* training — setting the loss function $\mathcal{L}_1$ as the MSE between the target parameters $\boldsymbol{\theta}$ from AAE and the output parameters $\hat{\boldsymbol{\theta}}$ from SuperEncoder. To evaluate the performance of $\mathcal{L}_1$, we train a SuperEncoder using MNIST dataset, and test if it could load a test digit image into a quantum state with high fidelity. All images are downsampled and normalized into 4-qubit states for quick evaluation.

Unfortunately, results in Table 2 show that $\mathcal{L}_1$ achieves poor performance. The average fidelity of prepared quantum states is only 0.6208. As demonstrated in Fig. 4, $\mathcal{L}_1$ generates a state that losses the patterns of the original state. Additionally, utilizing $\mathcal{L}_1$ implies that we need to first generate target parameters using AAE, of which the long runtime hinders pre-training on larger datasets. Consequently, required is a more effective loss function design without involving AAE.

$\mathcal{L}_1$	$\mathcal{L}_2$	$\mathcal{L}_3$
0.6208	0.9873	0.9908

Table 2: Fidelity comparison between SuperEncoders trained with different loss functions.

To address this challenge, we propose a *state-oriented* training methodology, which employs quantum states as targets to guide optimizations. Specifically, we may apply $\hat{\boldsymbol{\theta}}$ to the circuit and execute it to obtain the prepared state $\hat{\psi}$. Then it is possible to calculate the difference between $\hat{\psi}$ and ψ as the loss to optimize SuperEncoder. In contrast to parameter-oriented training, this approach applies to larger datasets as it decouples the training procedure from AAE. We utilize two different state-oriented metrics, the first being the MSE between $\hat{\psi}$ and ψ, denoted as $\mathcal{L}_2$, and the second is the *fidelity* of $\hat{\psi}$ relative to ψ, expressed as $\mathcal{L}_3 = 1 - |\langle\hat{\psi}|\psi\rangle|^2$ [25]. Results in Table 2 show that $\mathcal{L}_2$ and $\mathcal{L}_3$ achieve remarkably higher fidelity than $\mathcal{L}_1$. Besides, we observe that $\mathcal{L}_3$ prepares a state very similar to the target one (Fig. 4), verifying that state-oriented training is more effective than parameter-oriented training.

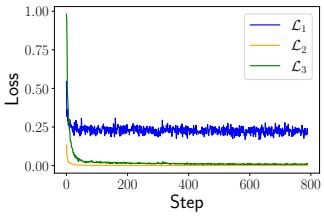

Figure 5: Convergence of different loss functions.

Landscape Analysis. To understand the efficacy of these loss functions, we further analyze their landscapes following previous studies [28, 40, 18]. To gain insight from the landscape, we plot Fig. 6 using the same scale and color gradients [18]. Compared to state-oriented losses ($\mathcal{L}_2$ and $\mathcal{L}_3$), $\mathcal{L}_1$ has a largely flat landscape with non-decreasing minima, thus the model struggles to explore a viable path towards a lower loss value, a similar pattern can also be observed in Fig. 5. In contrast, $\mathcal{L}_2$

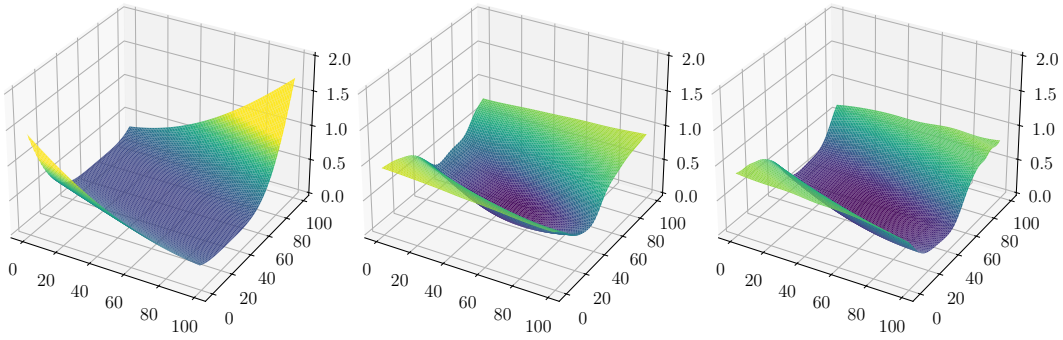

(a) $\mathcal{L}_1$ (b) $\mathcal{L}_2$ (c) $\mathcal{L}_3$

Figure 6: Landscape virtualization of different loss functions.

and $\mathcal{L}_3$ have much lower minima and successfully converge to smaller loss values. Furthermore, we observe from Fig. 6 that $\mathcal{L}_3$ has a wider minima than $\mathcal{L}_2$, which may indicate a better generalization capability [40].

Gradient Analysis. Based on the landscape analysis, we adopt $\mathcal{L}_3$ as the loss function to train SuperEncoder. We note that $\mathcal{L}_3$ can be written as $1 - \langle\psi|\hat{\psi}\rangle\langle\hat{\psi}|\psi\rangle$. If $\hat{\rho}$ is a pure state, it is equivalent to $|\hat{\psi}\rangle\langle\hat{\psi}|$. Then $\mathcal{L}_3$ is given by $\mathcal{L}_3 = 1 - \langle\psi|\hat{\rho}|\psi\rangle$.

This re-formalization is important as only the mixed state $\hat{\rho}$ could be obtained in noisy environments. Suppose an n-qubit circuit is parameterized by m parameters $\hat{\boldsymbol{\theta}} = [\hat{\theta}_1, \ldots, \hat{\theta}_k, \ldots, \hat{\theta}_m]$. Let $\mathbf{W}$ be the weight matrix of MLP, with k, l the element indices. We analyze the gradient of $\mathcal{L}_3$ w.r.t. $W_{k,l}$ to showcase its feasibility in different quantum computing environments.

$$
\begin{aligned}
\nabla_{W_{k,l}}\mathcal{L}_3 = \frac{\partial \mathcal{L}_3}{\partial W_{k,l}} &= -\langle\psi|\frac{\partial \hat{\rho}}{\partial W_{k,l}}|\psi\rangle \\
&= -\langle\psi| \begin{bmatrix} \sum_{j=1}^{m} \frac{\partial \hat{\rho}_{1,1}}{\partial \theta_j}\frac{\partial \theta_j}{\partial W_{k,l}} & \cdots & \sum_{j=1}^{m} \frac{\partial \hat{\rho}_{1,N}}{\partial \theta_j}\frac{\partial \theta_j}{\partial W_{k,l}} \\ \vdots & \ddots & \vdots \\ \sum_{j=1}^{m} \frac{\partial \hat{\rho}_{N,1}}{\partial \theta_j}\frac{\partial \theta_j}{\partial W_{k,l}} & \cdots & \sum_{j=1}^{m} \frac{\partial \hat{\rho}_{N,N}}{\partial \theta_j}\frac{\partial \theta_j}{\partial W_{k,l}} \end{bmatrix} |\psi\rangle,
\end{aligned} \tag{1}
$$

The calculation of $\frac{\partial \theta_j}{\partial W_{k,l}}$ can be easily done on classical devices using backpropagation supported by automatic differentiation frameworks. Therefore, we only focus on $\frac{\partial \hat{\rho}_{i,j}}{\partial \theta_k}$. In a simulation environment, the calculation of $\hat{\rho}$ is conducted via noisy quantum circuit simulation, which is essentially a series of tensor operations on state vectors. Therefore, the calculation of $\frac{\partial \hat{\rho}_{i,j}}{\partial \theta_k}$ is compatible with backpropagation. The situation on real devices becomes more complicated. On real devices, the mixed state $\hat{\rho}$ is reconstructed through *quantum tomography* [7] based on classical shadow [55, 16]. Here, for notion simplicity, we denote the process of classical shadow as a transformation $\mathcal{S}$, and denote the measurement expectations of the ansatz as $U(\hat{\boldsymbol{\theta}})$. Thus the reconstructed density matrix is given by $\hat{\rho} = \mathcal{S}(U(\hat{\boldsymbol{\theta}}))$. Then the gradient of $\hat{\rho}_{i,j}$ with respect to $\hat{\theta}_k$ is $\sum_u \frac{\partial \hat{\rho}_{i,j}}{\partial U(\hat{\boldsymbol{\theta}})}\frac{\partial U(\hat{\boldsymbol{\theta}})}{\partial \hat{\theta}_k}$. Here $\frac{\partial \hat{\rho}_{i,j}}{\partial U(\hat{\boldsymbol{\theta}})}$ can be efficiently calculated on classical devices using backpropagation, as $\mathcal{S}$ operates on expectation values on classical devices. However, $U(\hat{\boldsymbol{\theta}})$ involves state evolution on quantum devices, where back-propagation is impossible due to the No-Cloning theorem [36]. Fortunately, it is possible to utilize the *parameter shift* rule [8, 4, 53] to calculate $\frac{\partial U(\hat{\boldsymbol{\theta}})}{\partial \theta_k}$. In this way, the gradients of the circuit function U with respect to θ_j are $\frac{\partial U(\hat{\boldsymbol{\theta}})}{\partial \theta_k} = \frac{1}{2}\left(U(\theta_+) - U(\theta_-)\right)$, where $\theta_+ = [\theta_1, \ldots, \theta_k + \frac{\pi}{2}, \ldots, \theta_m], \theta_- = [\theta_1, \ldots, \theta_k - \frac{\pi}{2}, \ldots, \theta_m]$. To summarize, training SuperEncoder with $\mathcal{L}_3$ is theoretically feasible on both simulators and real devices.

4 Numerical Results

4.1 Experiment Setup

Datasets. To train a SuperEncoder for arbitrary quantum states, we need a dataset comprising a wide range of quantum states with different distributions. To our knowledge, there is no dataset dedicated for this special purpose. A natural solution is to use readily available datasets from classical machine learning domains (e.g., ImageNet [9], Places [58], SQuAD [44]) by normalizing them to quantum states. However, QSP is essential in various application scenarios besides QML. The classical data to be loaded may not only contain natural images or languages but also contain arbitrary data (e.g., in HHL algorithm [15]). Therefore, we construct a training dataset adapted from FractalDB-60 [21] with 60k samples, a formula-driven dataset originally designed for computer vision without any natural images. We also construct a separate dataset to test the performance of QSP, which consists of data sampled from different statistical distributions, including uniform, normal, log-normal, exponential, and Dirichlet distributions, with 3000 samples per distribution. Hereafter we refer this dataset as the *synthetic dataset*.

Platforms. We implement SuperEncoder using PennyLane [34], PyTorch [37] and Qiskit [43]. Simulations are done on a Ubuntu server with 768 GB memory, two 32-core Intel(R) Xeon(R) Silver 4216 CPU with 2.10 GHz, and 2 NVIDIA A-100 GPUs. IBM quantum cloud platform[2] is adopted to evaluate the performance on real quantum devices.

Metrics. We evaluate SuperEncoder and compare it to AE and AAE in terms of runtime, scalability, and fidelity. *Runtime* refers to how long it takes to prepare a quantum state. *Scalability* refers to how the circuit depth grows with the number of qubits. *Fidelity* evaluates the similarity between prepared quantum states and target quantum states. Specifically, the fidelity for two mixed states given by density matrices ρ and $\hat{\rho}$ is defined as $F(\rho, \hat{\rho}) = \mathrm{Tr}\left(\sqrt{\sqrt{\rho}\hat{\rho}\sqrt{\rho}}\right)^2 \in [0, 1]$. A larger F indicates a better fidelity.

Implementation. We implement SuperEncoder using an MLP consisting of two hidden layers. The dimensions of input and output layers are respectively set to 2^n and m, where n refers to the number of qubits and m refers to the number of parameters. We adopt $\mathcal{L}_3$ as the loss function. Training data are down-sampled, flattened, and normalized to 2^n-dimensional state vectors. We adopt the hardware efficient ansatz [20] (Fig. 2) as the backbone of quantum circuits and use the same structure for AAE. Given a target state, a pre-trained SuperEncoder model is invoked to generate parameters and thus the circuit for QSP. While for AAE, we employ online iterations for each state. For AE, the arithmetic decomposition method in PennyLane [34, 4] is adopted. We defer more details about implementation to Appendix A. Our framework is open-source at https://anonymous.4open.science/r/SuperEncoder-A733 with detailed instructions to reproduce our results.

4.2 Evaluation on Synthetic Dataset

For simplicity and without loss of generality, we focus our discussion on the results of 4-qubit QSP tasks. The outcomes for larger quantum states are detailed in Appendix B.1. The parameters of both AAE and SuperEncoder are optimized based on ideal quantum circuit simulation.

Runtime. The runtime and fidelity results, evaluated on the synthetic dataset, are presented in Table 3. We observe that SuperEncoder runs faster than AAE by orders of magnitudes and has a similar runtime to AE, affirming that SuperEncoder effectively overcomes the main drawback of AAE.

	AE		AAE		SuperEncoder	
	Fidelity	Runtime	Fidelity	Runtime	Fidelity	Runtime
Uniform			0.9996		0.9731	
Normal			0.9992		0.8201	
Log-normal			0.9993		0.9421	
Exponential			0.9996		0.9464	
Dirichlet			0.9995		0.9737	
Average	1.0000	0.0162 s	0.9994	5.0201 s	0.9310	0.0397 s

Table 3: Comparison between AE, AAE and SuperEncoder in terms of runtime and fidelity.

[2] https://quantum-computing.ibm.com/

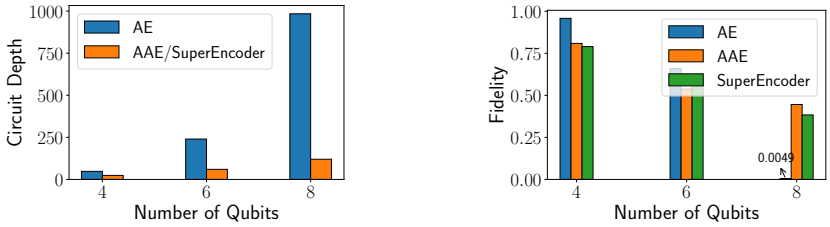

(a) Scaling of circuit depth w.r.t. # qubits. (b) Fidelity of different QSP methods on `ibm_osaka`.

Figure 7: Comparison between AE, AAE, and SuperEncoder in terms of circuit depth and fidelity on real devices.

Scalability. Although AE runs fast, it exhibits poor scalability since the circuit depth grows exponentially with the number of qubits. The depth of AAE is empirically determined by increasing depth until the final fidelity does not increase, same depth is adopted for SuperEncoder. We deter the details of determining the depth of AAE/SuperEncoder to Appendix A. As shown in Fig. 7a, the depth of AE grows fast and becomes much larger than AAE/SuperEncoder, e.g., the depth of AE for a 8-qubit state is 984, whereas the depth of AAE/SuperEncoder is only 120.

Fidelity. From Table 3, it is evident that SuperEncoder experiences notable fidelity degradation when compared with AAE and AE. Specifically, the average fidelity of SuperEncoder is 0.9307, whereas AAE and AE achieve higher average fidelities of 0.9994 and 1.0, respectively. Note that, although AE demonstrates the highest fidelity under ideal simulation, its performance deteriorates significantly in noisy environments. Fig. 7b presents the performance of these three QSP methods on quantum states with 4, 6, and 8 qubits on the `ibm_osaka` machine. While the fidelity of AE is higher than AAE/SuperEncoder on the 4-qubit and 6-qubit states, its fidelity on the 8-qubit state is only 0.0049, becoming much lower than AAE/SuperEncoder. This decline is primarily attributed to its large circuit depth as shown in Fig. 7a.

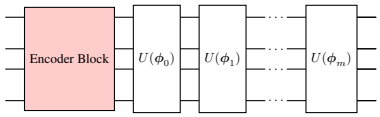

AE	AAE	SuperEncoder
97.15%	98.01%	97.87%

Figure 8: Schematic of a QNN (above) and test accuracies of QSP methods on the QML task (below).

4.3 Application to Downstream Tasks

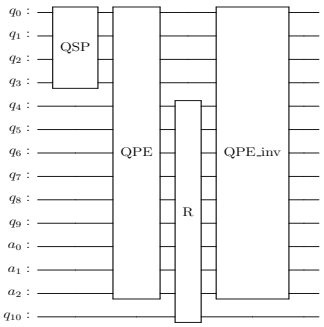

Figure 9: Schematic of HHL.

Quantum Machine Learning. We first apply SuperEncoder to a QML task. MNIST dataset is adopted for demonstration, we extract a sub-dataset composed on digits 3 and 6 for evaluation. The quantum circuit that implements a QNN is depicted in Fig. 8, which consists of an encoder block and m entangler layers. Here the encoder block is implemented via QSP circuits, either AE, AAE, or SuperEncoder, of which the parameters are frozen during the training of QNN. The test results are shown in Fig. 8, we observe that SuperEncoder achieves similar performance with AAE and AE. The reason lies in the fact that classification tasks can be robust to noises. Consequently, approximate QSP (AAE and SuperEncoder) with a certain degree of fidelity loss is tolerable.

HHL Algorithm. Besides QML, quantum-enhanced linear algebra algorithms are another important set of applications that heavily rely on QSP. The most famous algorithm is the HHL algorithm [15]. The problem can be defined as, given a matrix $\mathbf{A} \in \mathbb{C}^{N\times N}$, and a vector $\mathbf{b} \in \mathbb{C}^N$, find $\mathbf{x} \in \mathbb{C}^N$ satisfying $\mathbf{Ax} = \mathbf{b}$. A typical implementation of HHL utilizes the circuit depicted in Fig. 9. The outline of HHL is as follows. (i) Apply a QSP circuit to prepare the quantum state $|\mathbf{b}\rangle$. (ii) Apply Quantum Phase Estimation [10] (QPE) to estimate the eigenvalue of $\mathbf{A}$ (iii) Apply conditioned rotation gates on ancillary qubits based on the eigenvalues (R). (iv) Apply an inverse QPE (QPE_inv) and measure the ancillary qubits to reconstruct the solution vector $\mathbf{x}$. Note that, HHL does not return the solution $\mathbf{x}$ itself, but rather an approximation of the expectation value of some operator $\mathbf{M}$ associated with $\mathbf{x}$, e.g.,

$\mathbf{x}^\dagger\mathbf{M}\mathbf{x}$. Here, we adopt an optimized version of HHL proposed by Vazquez et al. [51] for evaluation. To compare the performance between different QSP methods, we construct linear equations with fixed matrix $\mathbf{A}$ and operator $\mathbf{M}$, while we sample different vectors from our synthetic dataset as $\mathbf{b}$. Results are concluded in Table 4. Unlike QML, HHL expects precise QSP, thus we take the results from AE as the ground truth values and compare the relative error between AAE/SuperEncoder and AE. The relative error of SuperEncoder is 2.4094%, while the error of AAE is only 0.3326%.

4.4 Discussion and Future Work

The results of our evaluation can be concluded in two folds. (i) SuperEncoder effectively eliminates the iteration overhead of AAE, thereby becoming both fast and scalable. However, it has a notable degradation in fidelity. (ii) The impact of fidelity degradation varies across different downstream applications. For QML, the fidelity degradation is affordable as long as the prepared states are distinguishable across different classes. However, algorithms like HHL rely on precise QSP to produce the best result. In these algorithms, SuperEncoder suffers from higher error ratio than AAE.

	AE	AAE	SuperEncoder
$\mathbf{b}_0$	0.7391	0.7404	0.7355
$\mathbf{b}_1$	0.7449	0.7445	0.7544
$\mathbf{b}_2$	0.7492	0.7469	0.8134
$\mathbf{b}_3$	0.7164	0.7099	0.7223
$\mathbf{b}_4$	0.7092	0.7076	0.7155
Avg err		0.3326%	2.4094%

Table 4: Performance of different QSP methods in HHL algorithm. 'Avg err' denotes the average relative errors between AAE/SuperEncoder and AE.

Note that, the current evaluation results may not reflect the actual performance of SuperEncoder on real NISQ devices. Recent work has shown that AAE achieves significantly better fidelity than AE does [52]. This is due to the intrinsic noise awareness of AAE, as it could obtain states from noisy devices to guide updating parameters with better robustness. In essence, the proposed SuperEncoder possesses the same nature as AAE. Unfortunately, although the noise-robustness of AAE can be evaluated on a small set of test samples, it is difficult to perform noise-aware training for SuperEncoder as it requires a large dataset for pre-training. Consequently, SuperEncoder relies on huge amounts of interactions with noisy devices, thereby becoming extremely time-consuming. As a result, the effectiveness of SuperEncoder in noisy environments remains largely unexplored, which we leave for future exploration. More discussion about this perspective is in Appendix C.

5 Related Work

Besides QSP, there are other methods for loading classical data into quantum states. These methods can be roughly regarded as *quantum feature embedding* primarily used in QML, which maps classical data to a completely different distribution encoded in quantum states. A widely used embedding method is known as angle embedding. Li et al. have proven that this method has a concentration issue, which means that the encoded states may become indistinguishable as the circuit depth increases [26]. Lei et al. proposed an automatic design framework for efficient quantum feature embedding, resolving the issue of concentration [24]. The central idea of this framework is to search for the most efficient circuit architecture for a given classical input, which is also known as Quantum Architecture Search (QAS) [38, 30, 54]. While the application scenario of quantum feature embedding is largely limited to QML, QSP has broader usage in general quantum applications, distinguishing SuperEncoder from all aforementioned work.

6 Conclusion

In this work, we propose SuperEncoder, a neural network-based QSP framework. Instead of iteratively tuning the circuit parameters to approximate each quantum state, as is done in AAE, we adopt a different approach by directly learning the relationship between target quantum states and the required circuit parameters. SuperEncoder combines the scalable circuit architecture of AAE with the fast runtime of AE, as verified by a comprehensive evaluation on both synthetic dataset and downstream applications.

References

[1] Amira Abbas, David Sutter, Christa Zoufal, Aurélien Lucchi, Alessio Figalli, and Stefan Woerner. The power of quantum neural networks. *Nature Computational Science*, 1(6):403–409, 2021.

[2] Israel F Araujo, Daniel K Park, Teresa B Ludermir, Wilson R Oliveira, Francesco Petruccione, and Adenilton J Da Silva. Configurable sublinear circuits for quantum state preparation. *Quantum Information Processing*, 22(2):123, 2023.

[3] Johannes Bausch. Recurrent quantum neural networks. *Advances in neural information processing systems*, 33:1368–1379, 2020.

[4] Ville Bergholm, Josh Izaac, Maria Schuld, Christian Gogolin, Shahnawaz Ahmed, Vishnu Ajith, M Sohaib Alam, Guillermo Alonso-Linaje, B AkashNarayanan, Ali Asadi, et al. Pennylane: Automatic differentiation of hybrid quantum-classical computations. *arXiv preprint arXiv:1811.04968*, 2018.

[5] Jacob Biamonte, Peter Wittek, Nicola Pancotti, Patrick Rebentrost, Nathan Wiebe, and Seth Lloyd. Quantum machine learning. *Nature*, 549(7671):195–202, 2017.

[6] Tianping Chen and Hong Chen. Universal approximation to nonlinear operators by neural networks with arbitrary activation functions and its application to dynamical systems. *IEEE Transactions on Neural Networks*, 6(4):911–917, 1995.

[7] Marcus Cramer, Martin B Plenio, Steven T Flammia, Rolando Somma, David Gross, Stephen D Bartlett, Olivier Landon-Cardinal, David Poulin, and Yi-Kai Liu. Efficient quantum state tomography. *Nature communications*, 1(1):149, 2010.

[8] Gavin E Crooks. Gradients of parameterized quantum gates using the parameter-shift rule and gate decomposition. *arXiv preprint arXiv:1905.13311*, 2019.

[9] Jia Deng, Wei Dong, Richard Socher, Li-Jia Li, Kai Li, and Li Fei-Fei. Imagenet: A large-scale hierarchical image database. In *2009 IEEE conference on computer vision and pattern recognition*, pages 248–255. Ieee, 2009.

[10] Uwe Dorner, Rafal Demkowicz-Dobrzanski, Brian J Smith, Jeff S Lundeen, Wojciech Wasilewski, Konrad Banaszek, and Ian A Walmsley. Optimal quantum phase estimation. *Physical review letters*, 102(4):040403, 2009.

[11] Edward Farhi, Jeffrey Goldstone, and Sam Gutmann. A quantum approximate optimization algorithm. *arXiv preprint arXiv:1411.4028*, 2014. https://doi.org/10.48550/arXiv.1411.4028.

[12] Niels Gleinig and Torsten Hoefler. An efficient algorithm for sparse quantum state preparation. In *2021 58th ACM/IEEE Design Automation Conference (DAC)*, pages 433–438. IEEE, 2021.

[13] Javier Gonzalez-Conde, Ángel Rodríguez-Rozas, Enrique Solano, and Mikel Sanz. Simulating option price dynamics with exponential quantum speedup. *arXiv preprint arXiv:2101.04023*, 2021.

[14] Javier Gonzalez-Conde, Thomas W Watts, Pablo Rodriguez-Grasa, and Mikel Sanz. Efficient quantum amplitude encoding of polynomial functions. *Quantum*, 8:1297, 2024.

[15] Aram W Harrow, Avinatan Hassidim, and Seth Lloyd. Quantum algorithm for linear systems of equations. *Physical Review Letters*, 103(15):150502, 2009. https://doi.org/10.1103/PhysRevLett.103.150502.

[16] Hsin-Yuan Huang. Learning quantum states from their classical shadows. *Nature Reviews Physics*, 4(2):81–81, 2022.

[17] Jason Iaconis, Sonika Johri, and Elton Yechao Zhu. Quantum state preparation of normal distributions using matrix product states. *npj Quantum Information*, 10(1):15, 2024.

[18] Christian Cmehil-Warn Jacob Hansen. Loss landscapes. In *ICLR Blog Track*, 2022. https://loss-landscapes.github.io/Loss-Landscapes-Blog/2022/12/01/loss-landscapes/.

[19] Weiwen Jiang, Jinjun Xiong, and Yiyu Shi. A co-design framework of neural networks and quantum circuits towards quantum advantage. *Nature Communications*, 12(1):579, 2021. https://doi.org/10.1038/s41467-020-20729-5.

[20] Abhinav Kandala, Antonio Mezzacapo, Kristan Temme, Maika Takita, Markus Brink, Jerry M. Chow, and Jay M. Gambetta. Hardware-efficient variational quantum eigensolver for small molecules and quantum magnets. *Nature*, 549(7671):242–246, September 2017.

[21] Hirokatsu Kataoka, Kazushige Okayasu, Asato Matsumoto, Eisuke Yamagata, Ryosuke Yamada, Nakamasa Inoue, Akio Nakamura, and Yutaka Satoh. Pre-training without natural images. In *Proceedings of the Asian Conference on Computer Vision*, 2020.

[22] Diederik P Kingma and Jimmy Ba. Adam: A method for stochastic optimization. *arXiv preprint arXiv:1412.6980*, 2014.

[23] Philip Krantz, Morten Kjaergaard, Fei Yan, Terry P Orlando, Simon Gustavsson, and William D Oliver. A quantum engineer's guide to superconducting qubits. *Applied physics reviews*, 6(2), 2019.

[24] Cong Lei, Yuxuan Du, Peng Mi, Jun Yu, and Tongliang Liu. Neural auto-designer for enhanced quantum kernels. In *The Twelfth International Conference on Learning Representations*, 2023.

[25] Nelson Leung, Mohamed Abdelhafez, Jens Koch, and David Schuster. Speedup for quantum optimal control from automatic differentiation based on graphics processing units. *Physical Review A*, 95(4):042318, 2017. https://doi.org/10.1103/PhysRevA.95.042318.

[26] Guangxi Li, Ruilin Ye, Xuanqiang Zhao, and Xin Wang. Concentration of data encoding in parameterized quantum circuits. *Advances in Neural Information Processing Systems*, 35:19456–19469, 2022.

[27] Gushu Li, Yufei Ding, and Yuan Xie. Tackling the qubit mapping problem for nisq-era quantum devices. In *Proceedings of the Twenty-Fourth International Conference on Architectural Support for Programming Languages and Operating Systems*, pages 1001–1014, 2019. https://doi.org/10.1145/3297858.3304023.

[28] Hao Li, Zheng Xu, Gavin Taylor, Christoph Studer, and Tom Goldstein. Visualizing the loss landscape of neural nets. *Advances in neural information processing systems*, 31, 2018.

[29] Gui-Lu Long and Yang Sun. Efficient scheme for initializing a quantum register with an arbitrary superposed state. *Physical Review A*, 64(1):014303, 2001.

[30] Xudong Lu, Kaisen Pan, Ge Yan, Jiaming Shan, Wenjie Wu, and Junchi Yan. Qas-bench: rethinking quantum architecture search and a benchmark. In *International Conference on Machine Learning*, pages 22880–22898. PMLR, 2023.

[31] Michael Lubasch, Jaewoo Joo, Pierre Moinier, Martin Kiffner, and Dieter Jaksch. Variational quantum algorithms for nonlinear problems. *Physical Review A*, 101(1):010301, 2020.

[32] Rui Mao, Guojing Tian, and Xiaoming Sun. Towards optimal circuit size for sparse quantum state preparation. *arXiv e-prints*, pages arXiv–2404, 2024.

[33] Kosuke Mitarai, Makoto Negoro, Masahiro Kitagawa, and Keisuke Fujii. Quantum circuit learning. *Physical Review A*, 98(3):032309, 2018.

[34] Mikko Möttönen, JJ Vartiainen, Ville Bergholm, and Martti M Salomaa. Transformation of quantum states using uniformly controlled rotations. *Quantum Information and Computation*, 5, 2005.

[35] Kouhei Nakaji, Shumpei Uno, Yohichi Suzuki, Rudy Raymond, Tamiya Onodera, Tomoki Tanaka, Hiroyuki Tezuka, Naoki Mitsuda, and Naoki Yamamoto. Approximate amplitude encoding in shallow parameterized quantum circuits and its application to financial market indicators. *Physical Review Research*, 4(2):023136, 2022.

[36] Michael A Nielsen and Isaac L Chuang. Quantum computation and quantum information. 2010.

[37] Adam Paszke, Sam Gross, Francisco Massa, Adam Lerer, James Bradbury, Gregory Chanan, Trevor Killeen, Zeming Lin, Natalia Gimelshein, Luca Antiga, et al. Pytorch: An imperative style, high-performance deep learning library. *Advances in neural information processing systems*, 32, 2019.

[38] Yash J. Patel, Akash Kundu, Mateusz Ostaszewski, Xavier Bonet-Monroig, Vedran Dunjko, and Onur Danaci. Curriculum reinforcement learning for quantum architecture search under hardware errors. In *The Twelfth International Conference on Learning Representations*, 2024.

[39] Alberto Peruzzo, Jarrod McClean, Peter Shadbolt, Man-Hong Yung, Xiao-Qi Zhou, Peter J Love, Alán Aspuru-Guzik, and Jeremy L O'brien. A variational eigenvalue solver on a photonic quantum processor. *Nature communications*, 5(1):4213, 2014. https://doi.org/10.1038/ncomms5213.

[40] Henning Petzka, Michael Kamp, Linara Adilova, Cristian Sminchisescu, and Mario Boley. Relative flatness and generalization. *Advances in neural information processing systems*, 34:18420–18432, 2021.

[41] Martin Plesch and Časlav Brukner. Quantum-state preparation with universal gate decompositions. *Physical Review A*, 83(3):032302, 2011.

[42] John Preskill. Quantum computing in the NISQ era and beyond. *Quantum*, 2:79, 2018.

[43] Qiskit contributors. Qiskit: An open-source framework for quantum computing, 2023.

[44] Pranav Rajpurkar, Jian Zhang, Konstantin Lopyrev, and Percy Liang. Squad: 100,000+ questions for machine comprehension of text. *arXiv preprint arXiv:1606.05250*, 2016.

[45] Maria Schuld, Ilya Sinayskiy, and Francesco Petruccione. Prediction by linear regression on a quantum computer. *Physical Review A*, 94(2):022342, 2016.

[46] Vivek V Shende, Stephen S Bullock, and Igor L Markov. Synthesis of quantum logic circuits. In *Proceedings of the 2005 Asia and South Pacific Design Automation Conference*, pages 272–275, 2005.

[47] Peter W Shor. Polynomial-time algorithms for prime factorization and discrete logarithms on a quantum computer. *SIAM review*, 41(2):303–332, 1999. https://doi.org/10.1137/S0036144598347011.

[48] Siddarth Srinivasan, Carlton Downey, and Byron Boots. Learning and inference in hilbert space with quantum graphical models. *Advances in Neural Information Processing Systems*, 31, 2018.

[49] Xiaoming Sun, Guojing Tian, Shuai Yang, Pei Yuan, and Shengyu Zhang. Asymptotically optimal circuit depth for quantum state preparation and general unitary synthesis. *IEEE Transactions on Computer-Aided Design of Integrated Circuits and Systems*, 2023.

[50] Jinkai Tian, Xiaoyu Sun, Yuxuan Du, Shanshan Zhao, Qing Liu, Kaining Zhang, Wei Yi, Wanrong Huang, Chaoyue Wang, Xingyao Wu, et al. Recent advances for quantum neural networks in generative learning. *IEEE Transactions on Pattern Analysis and Machine Intelligence*, 2023.

[51] Almudena Carrera Vazquez, Ralf Hiptmair, and Stefan Woerner. Enhancing the quantum linear systems algorithm using richardson extrapolation. *ACM Transactions on Quantum Computing*, 3(1):1–37, 2022.

[52] Hanrui Wang, Yilian Liu, Pengyu Liu, Jiaqi Gu, Zirui Li, Zhiding Liang, Jinglei Cheng, Yongshan Ding, Xuehai Qian, Yiyu Shi, et al. Robuststate: Boosting fidelity of quantum state preparation via noise-aware variational training. *arXiv preprint arXiv:2311.16035*, 2023.

[53] David Wierichs, Josh Izaac, Cody Wang, and Cedric Yen-Yu Lin. General parameter-shift rules for quantum gradients. *Quantum*, 6:677, 2022.

[54] Wenjie Wu, Ge Yan, Xudong Lu, Kaisen Pan, and Junchi Yan. Quantumdarts: differentiable quantum architecture search for variational quantum algorithms. In *International Conference on Machine Learning*, pages 37745–37764. PMLR, 2023.

[55] Ting Zhang, Jinzhao Sun, Xiao-Xu Fang, Xiao-Ming Zhang, Xiao Yuan, and He Lu. Experimental quantum state measurement with classical shadows. *Physical Review Letters*, 127(20):200501, 2021.

[56] Xiao-Ming Zhang, Man-Hong Yung, and Xiao Yuan. Low-depth quantum state preparation. *Physical Review Research*, 3(4):043200, 2021.

[57] Jian Zhao, Yu-Chun Wu, Guang-Can Guo, and Guo-Ping Guo. State preparation based on quantum phase estimation. *arXiv preprint arXiv:1912.05335*, 2019.

[58] Bolei Zhou, Agata Lapedriza, Aditya Khosla, Aude Oliva, and Antonio Torralba. Places: A 10 million image database for scene recognition. *IEEE transactions on pattern analysis and machine intelligence*, 40(6):1452–1464, 2017.

[59] Christa Zoufal, Aurélien Lucchi, and Stefan Woerner. Quantum generative adversarial networks for learning and loading random distributions. *npj Quantum Information*, 5(1):103, 2019.

The structure of our Appendix is as follows. Appendix A provides more details of implementing SuperEncoder. Appendix B provides additional numerical results to illustrate the impact of state sizes, model architectures, and training datasets. Appendix C analyzes the estimated runtime of training SuperEncoder on real devices.

A Implementation Details

In this section, we elaborate the missing details of SuperEncoder in the main text.

The overarching workflow of SuperEncoder is illustrated in Fig. 10. The target quantum states are input to the MLP model. Then, the MLP model generates predicted parameters based on the target states. Afterwards, the parameters are applied to the PQC to obtain the prepared quantum states. Finally, we calculate the loss based on the prepared states and target states and optimize the weights of MLP through backpropagation.

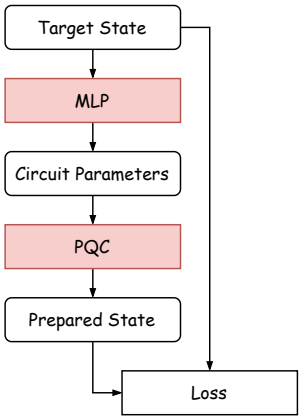

Figure 10: Detailed workflow of SuperEncoder.

The settings of MLP and PQC are as follows.

MLP. As listed in Table 5, we implement a two-layer MLP. Each layer consists of 512 neurons. We employ `Tanh` as the activation functions since $\boldsymbol{\theta}$ represents the *angles* of rotation gates, ranging from $-\pi$ to π.

Linear	Input	$(\text{batch\_size},\ 2^n)$
	Output	$(\text{batch\_size},\ 512)$
Tanh	Input	$(\text{batch\_size},\ 512)$
	Output	$(\text{batch\_size},\ 512)$
Linear	Input	$(\text{batch\_size},\ 512)$
	Output	$(\text{batch\_size},\ \dim(\boldsymbol{\theta}))$
Tanh	Input	$(\text{batch\_size},\ \dim(\boldsymbol{\theta}))$
	Output	$(\text{batch\_size},\ \dim(\boldsymbol{\theta}))$

Table 5: MLP based SuperEncoder. n refers to the number of qubits. $\boldsymbol{\theta}$ denotes the parameter vector.

PQC. The circuit structure is the same with the one depicted in Fig. 2, except that the number of blocks is determined dynamically through empirical examinations. Specifically, we utilize AAE to approximate a target state while increasing the number of blocks. The number of blocks is designated when the resulting state fidelity no longer increases. For example, Fig. 11 demonstrates how fidelity changes while increasing the number of blocks. As one can observe, the fidelity converges when the number of layers is larger than 8. Hence, the number of layers is set to be 8 for 4-qubit quantum states. We follow the same procedure to set the number of blocks for other state sizes. Each block has the same structure, consisting of a rotation layer and an entangler layer. Given an n-qubit system, a rotation layer comprises n R_y gates, each operating on a distinct qubit. The entangler layer is composed of two CNOT layers. The first CNOT layer applies CNOT gates to $\{(q_0, q_1), (q_2, q_3), \dots\}$, and the second CNOT layer applies CNOT gates to $\{(q_1, q_2), (q_3, q_4), \dots\}$. Hence, the depth of

a block is 3. Let l be the number of blocks; then the dimension of the parameter vector is given by $\dim(\boldsymbol{\theta}) = n \times l$, and the depth of AAE/SuperEncoder is $3 \times l$. We conclude the settings of AAE/SuperEncoder used throughout this study in Table 6.

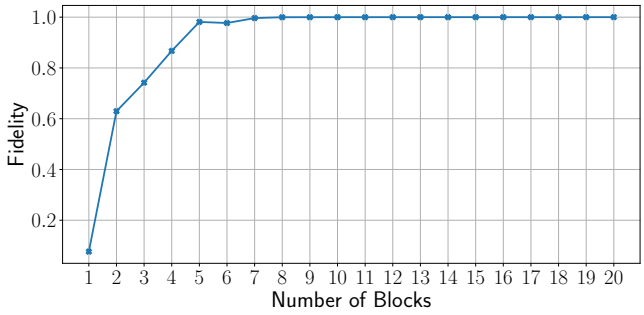

Figure 11: Fidelity vs. # blocks for 4-qubit states using AAE.

Number of Qubits	4	6	8
Number of Blocks	8	20	40
Depth	24	60	120

Table 6: Number of blocks and corresponding depth of AAE/SuperEncoder.

The hyperparameters for training SuperEncoder and optimizing AAE are as follows.

Training Hyperparameters for SuperEncoder. Throughout our experiments, the number of epochs are consistently set to be 10. For 4-qubit states, we set `bath_size` to 32, while we set it 64 for 6-qubit and 8-qubit states. We adopt Adam optimizer [22] with a learning rate of 3e-3 and a weight decay of 1e-5.

Hyperparameters for AAE. To optimize the parameters of AAE, we also use the Adam optimizer, with a learning rate of 1e-2 and zero weight decay. For all quantum states, we train the AAE for 100 steps.

B More Numerical Results

B.1 Results on Larger Quantum States

In line with the main text, we train the SuperEncoder for 6-qubit and 8-qubit quantum states using FractalDB-60 as the training dataset. Then we evaluate the performance of SuperEncoder on the synthetic test datasets. As shown in Table 7, the average fidelity on 6-qubit and 8-qubit states are 0.8655 and 0.7624 respectively. In Appendix B.2, B.3, we discuss potential optimizations to alleviate this performance degradation.

Dataset	$n = 4$	$n = 6$	$n = 8$
Uniform	0.9731	0.9254	0.8648
Normal	0.8201	0.7457	0.6075
Log-normal	0.9421	0.8575	0.7122
Exponential	0.9464	0.8757	0.7613
Dirichlet	0.9737	0.9232	0.8663
Avg	0.9310	0.8655	0.7624
Avg-AAE	0.9994	0.9964	0.9910

Table 7: Performance evaluation on larger quantum states (6-qubit and 8-qubit). The last separate row shows the results of AAE for comparison.

B.2 Impact of Model Architecture

As a preliminary investigation, the optimal model architecture for SuperEncoder still requires further exploration. Currently, we have set the size of the hidden units at a constant 512 (Table 5). However, as the number of qubits, n, increases, a wider network architecture may become necessary. To showcase the impact of model width, we adjust the size to 4×2^n for 6-qubit states and 16×2^n for 8-qubit states, and compare their performance with the original settings, as shown in Table 8. As evident from the results, this simple adjustment significantly enhances the fidelity of SuperEncoder, suggesting that there is substantial potential to boost SuperEncoder's performance by developing a more tailored network architecture.

	$n = 6$		$n = 8$	
Dataset	$h = 512$	$h = 4 \times 2^6$	$h = 512$	$h = 16 \times 2^8$
Uniform	0.9254	**0.9267**	0.8648	**0.8821**
Normal	0.7457	**0.7580**	0.6075	**0.6401**
Log-normal	0.8575	**0.8608**	0.7122	**0.7294**
Exponential	**0.8757**	0.8732	0.7613	**0.7781**
Dirichlet	0.9232	**0.9261**	0.8663	**0.8805**
Avg	0.8655	**0.8690**	0.7624	**0.7820**

Table 8: Impact of increasing network width. Here h refers to the size of hidden units.

B.3 Impact of Training Datasets

In addition to refining the model architecture, the development of a specially designed dataset for pre-training SuperEncoder is essential. Currently, the dataset utilized is FractalDB [21], which is originally designed for computer vision tasks. However, given the wide range of applications of QSP, there is a need to accommodate diverse types of classical data from various domains. Therefore, how to create a comprehensive dataset that could fully unleash the potential of SuperEncoder remains an open question. While developing a pre-trained model that performs well in all kinds of applications may be challenging, we advocate for a strategy that combines pre-training with fine-tuning for the practical deployment of SuperEncoder, similar to the approach used with foundation models in classical machine learning. To substantiate this approach, we have compiled a separate dataset that encompasses a variety of statistical distributions not limited to those utilized for evaluation (but with different settings). As demonstrated in Table 9, after fine-tuning, the performance of SuperEncoder improves by approximately 0.03.

Dataset	Pre-training	Pre-training+Finetuning
Uniform	0.9731	**0.9909**
Normal	0.8201	**0.8879**
Log-normal	0.9421	**0.9717**
Exponential	0.9464	**0.9729**
Dirichlet	0.9737	**0.9903**
Avg	0.9310	**0.9627**

Table 9: Fidelity improvements after fine-tuning SuperEncoder using a dataset consisting of different distributions.

C Runtime Estimation for Training on Real Devices

Although we have theoretically analyzed the feasibility of training SuperEncoder using states from real devices (Section 3.2), its practical implementation poses significant challenges. Specifically, state-of-the-art quantum tomography techniques, such as classical shadow [55, 16], require numerous *snapshots*, each measuring a distinct observable.

To train SuperEncoder, each sample in the training dataset necessitates one classical shadow to obtain the prepared state. For instance, with the FractalDB-60 dataset, one training epoch requires 60,000 classical shadows. Our experiments on the IBM cloud platform reveal an average runtime of 3.02

seconds per circuit job excluding queuing time. Suppose the number of snapshots is 1000, then the total runtime to train SuperEncoder for 10 epochs is about 1,812,000,000 seconds[3], roughly 57 years, making the process prohibitively expensive and time-consuming.

However, quantum tomography is under active investigation, and we expect more efficient techniques to emerge for acquiring noisy quantum states from real devices. Additionally, with the advancement of quantum computing system, future systems may have tightly integrated quantum-classical heterogeneous architectures (shorter runtime per job) while being capable of executing numerous quantum circuits in parallel (jobs within a classical shadow can execute in parallel). Hence, we anticipate the training of SuperEncoder to be feasible in the future.

[3] $10 \times 1000 \times 60000 \times 3.02$

NeurIPS Paper Checklist

1. **Claims**

   Question: Do the main claims made in the abstract and introduction accurately reflect the paper's contributions and scope?

   Answer: [Yes]

   Justification: This work aims at training-free approximate quantum state preparation. As claimed in the abstract and introduction.

   Guidelines:

   - The answer NA means that the abstract and introduction do not include the claims made in the paper.
   - The abstract and/or introduction should clearly state the claims made, including the contributions made in the paper and important assumptions and limitations. A No or NA answer to this question will not be perceived well by the reviewers.
   - The claims made should match theoretical and experimental results, and reflect how much the results can be expected to generalize to other settings.
   - It is fine to include aspirational goals as motivation as long as it is clear that these goals are not attained by the paper.

2. **Limitations**

   Question: Does the paper discuss the limitations of the work performed by the authors?

   Answer: [Yes]

   Justification: SuperEncoder sacrifices fidelity, as discussed in Section 4.4.

   Guidelines:

   - The answer NA means that the paper has no limitation while the answer No means that the paper has limitations, but those are not discussed in the paper.
   - The authors are encouraged to create a separate "Limitations" section in their paper.
   - The paper should point out any strong assumptions and how robust the results are to violations of these assumptions (e.g., independence assumptions, noiseless settings, model well-specification, asymptotic approximations only holding locally). The authors should reflect on how these assumptions might be violated in practice and what the implications would be.
   - The authors should reflect on the scope of the claims made, e.g., if the approach was only tested on a few datasets or with a few runs. In general, empirical results often depend on implicit assumptions, which should be articulated.
   - The authors should reflect on the factors that influence the performance of the approach. For example, a facial recognition algorithm may perform poorly when image resolution is low or images are taken in low lighting. Or a speech-to-text system might not be used reliably to provide closed captions for online lectures because it fails to handle technical jargon.
   - The authors should discuss the computational efficiency of the proposed algorithms and how they scale with dataset size.
   - If applicable, the authors should discuss possible limitations of their approach to address problems of privacy and fairness.
   - While the authors might fear that complete honesty about limitations might be used by reviewers as grounds for rejection, a worse outcome might be that reviewers discover limitations that aren't acknowledged in the paper. The authors should use their best judgment and recognize that individual actions in favor of transparency play an important role in developing norms that preserve the integrity of the community. Reviewers will be specifically instructed to not penalize honesty concerning limitations.

3. **Theory Assumptions and Proofs**

   Question: For each theoretical result, does the paper provide the full set of assumptions and a complete (and correct) proof?

   Answer: [Yes]

Justification: All these necessary contents for theoretical results are included in Section 3.2.

Guidelines:

- The answer NA means that the paper does not include theoretical results.
- All the theorems, formulas, and proofs in the paper should be numbered and cross-referenced.
- All assumptions should be clearly stated or referenced in the statement of any theorems.
- The proofs can either appear in the main paper or the supplemental material, but if they appear in the supplemental material, the authors are encouraged to provide a short proof sketch to provide intuition.
- Inversely, any informal proof provided in the core of the paper should be complemented by formal proofs provided in appendix or supplemental material.
- Theorems and Lemmas that the proof relies upon should be properly referenced.

4. **Experimental Result Reproducibility**

Question: Does the paper fully disclose all the information needed to reproduce the main experimental results of the paper to the extent that it affects the main claims and/or conclusions of the paper (regardless of whether the code and data are provided or not)?

Answer: [Yes]

Justification: Our code is open-source with instructions to reproduce our results, as described in Section 4.1. We also describe the details of experiment settings in Appendix A.

Guidelines:

- The answer NA means that the paper does not include experiments.
- If the paper includes experiments, a No answer to this question will not be perceived well by the reviewers: Making the paper reproducible is important, regardless of whether the code and data are provided or not.
- If the contribution is a dataset and/or model, the authors should describe the steps taken to make their results reproducible or verifiable.
- Depending on the contribution, reproducibility can be accomplished in various ways. For example, if the contribution is a novel architecture, describing the architecture fully might suffice, or if the contribution is a specific model and empirical evaluation, it may be necessary to either make it possible for others to replicate the model with the same dataset, or provide access to the model. In general. releasing code and data is often one good way to accomplish this, but reproducibility can also be provided via detailed instructions for how to replicate the results, access to a hosted model (e.g., in the case of a large language model), releasing of a model checkpoint, or other means that are appropriate to the research performed.
- While NeurIPS does not require releasing code, the conference does require all submissions to provide some reasonable avenue for reproducibility, which may depend on the nature of the contribution. For example
  (a) If the contribution is primarily a new algorithm, the paper should make it clear how to reproduce that algorithm.
  (b) If the contribution is primarily a new model architecture, the paper should describe the architecture clearly and fully.
  (c) If the contribution is a new model (e.g., a large language model), then there should either be a way to access this model for reproducing the results or a way to reproduce the model (e.g., with an open-source dataset or instructions for how to construct the dataset).
  (d) We recognize that reproducibility may be tricky in some cases, in which case authors are welcome to describe the particular way they provide for reproducibility. In the case of closed-source models, it may be that access to the model is limited in some way (e.g., to registered users), but it should be possible for other researchers to have some path to reproducing or verifying the results.

5. **Open access to data and code**

Question: Does the paper provide open access to the data and code, with sufficient instructions to faithfully reproduce the main experimental results, as described in supplemental material?

Answer: [Yes]

Justification: See Section 4.1.

Guidelines:

- The answer NA means that paper does not include experiments requiring code.
- Please see the NeurIPS code and data submission guidelines (https://nips.cc/public/guides/CodeSubmissionPolicy) for more details.
- While we encourage the release of code and data, we understand that this might not be possible, so "No" is an acceptable answer. Papers cannot be rejected simply for not including code, unless this is central to the contribution (e.g., for a new open-source benchmark).
- The instructions should contain the exact command and environment needed to run to reproduce the results. See the NeurIPS code and data submission guidelines (https://nips.cc/public/guides/CodeSubmissionPolicy) for more details.
- The authors should provide instructions on data access and preparation, including how to access the raw data, preprocessed data, intermediate data, and generated data, etc.
- The authors should provide scripts to reproduce all experimental results for the new proposed method and baselines. If only a subset of experiments are reproducible, they should state which ones are omitted from the script and why.
- At submission time, to preserve anonymity, the authors should release anonymized versions (if applicable).
- Providing as much information as possible in supplemental material (appended to the paper) is recommended, but including URLs to data and code is permitted.

6. **Experimental Setting/Details**

Question: Does the paper specify all the training and test details (e.g., data splits, hyperparameters, how they were chosen, type of optimizer, etc.) necessary to understand the results?

Answer: [Yes]

Justification: We illustrate the experimental settings in Section 4.1, and provides additional details in Appendix A.

Guidelines:

- The answer NA means that the paper does not include experiments.
- The experimental setting should be presented in the core of the paper to a level of detail that is necessary to appreciate the results and make sense of them.
- The full details can be provided either with the code, in appendix, or as supplemental material.

7. **Experiment Statistical Significance**

Question: Does the paper report error bars suitably and correctly defined or other appropriate information about the statistical significance of the experiments?

Answer: [No]

Justification: Throughout our experiments, we set the random seed to be fixed for all libraries we used.

Guidelines:

- The answer NA means that the paper does not include experiments.
- The authors should answer "Yes" if the results are accompanied by error bars, confidence intervals, or statistical significance tests, at least for the experiments that support the main claims of the paper.
- The factors of variability that the error bars are capturing should be clearly stated (for example, train/test split, initialization, random drawing of some parameter, or overall run with given experimental conditions).
- The method for calculating the error bars should be explained (closed form formula, call to a library function, bootstrap, etc.)
- The assumptions made should be given (e.g., Normally distributed errors).

- It should be clear whether the error bar is the standard deviation or the standard error of the mean.
- It is OK to report 1-sigma error bars, but one should state it. The authors should preferably report a 2-sigma error bar than state that they have a 96% CI, if the hypothesis of Normality of errors is not verified.
- For asymmetric distributions, the authors should be careful not to show in tables or figures symmetric error bars that would yield results that are out of range (e.g. negative error rates).
- If error bars are reported in tables or plots, The authors should explain in the text how they were calculated and reference the corresponding figures or tables in the text.

8. **Experiments Compute Resources**

   Question: For each experiment, does the paper provide sufficient information on the computer resources (type of compute workers, memory, time of execution) needed to reproduce the experiments?

   Answer: [Yes]

   Justification: We describe the computer resources used in this paper in Section 4.1.

   Guidelines:

   - The answer NA means that the paper does not include experiments.
   - The paper should indicate the type of compute workers CPU or GPU, internal cluster, or cloud provider, including relevant memory and storage.
   - The paper should provide the amount of compute required for each of the individual experimental runs as well as estimate the total compute.
   - The paper should disclose whether the full research project required more compute than the experiments reported in the paper (e.g., preliminary or failed experiments that didn't make it into the paper).

9. **Code Of Ethics**

   Question: Does the research conducted in the paper conform, in every respect, with the NeurIPS Code of Ethics https://neurips.cc/public/EthicsGuidelines?

   Answer: [Yes]

   Justification: We have read the code of ethics and followed its requirements.

   Guidelines:

   - The answer NA means that the authors have not reviewed the NeurIPS Code of Ethics.
   - If the authors answer No, they should explain the special circumstances that require a deviation from the Code of Ethics.
   - The authors should make sure to preserve anonymity (e.g., if there is a special consideration due to laws or regulations in their jurisdiction).

10. **Broader Impacts**

    Question: Does the paper discuss both potential positive societal impacts and negative societal impacts of the work performed?

    Answer: [NA]

    Justification: This work has no societal impact.

    Guidelines:

    - The answer NA means that there is no societal impact of the work performed.
    - If the authors answer NA or No, they should explain why their work has no societal impact or why the paper does not address societal impact.
    - Examples of negative societal impacts include potential malicious or unintended uses (e.g., disinformation, generating fake profiles, surveillance), fairness considerations (e.g., deployment of technologies that could make decisions that unfairly impact specific groups), privacy considerations, and security considerations.

- The conference expects that many papers will be foundational research and not tied to particular applications, let alone deployments. However, if there is a direct path to any negative applications, the authors should point it out. For example, it is legitimate to point out that an improvement in the quality of generative models could be used to generate deepfakes for disinformation. On the other hand, it is not needed to point out that a generic algorithm for optimizing neural networks could enable people to train models that generate Deepfakes faster.
- The authors should consider possible harms that could arise when the technology is being used as intended and functioning correctly, harms that could arise when the technology is being used as intended but gives incorrect results, and harms following from (intentional or unintentional) misuse of the technology.
- If there are negative societal impacts, the authors could also discuss possible mitigation strategies (e.g., gated release of models, providing defenses in addition to attacks, mechanisms for monitoring misuse, mechanisms to monitor how a system learns from feedback over time, improving the efficiency and accessibility of ML).

11. **Safeguards**

    Question: Does the paper describe safeguards that have been put in place for responsible release of data or models that have a high risk for misuse (e.g., pretrained language models, image generators, or scraped datasets)?

    Answer: [NA]

    Justification: This paper poses no such risks as our released model and datasets are only able to be used for quantum state preparation.

    Guidelines:

    - The answer NA means that the paper poses no such risks.
    - Released models that have a high risk for misuse or dual-use should be released with necessary safeguards to allow for controlled use of the model, for example by requiring that users adhere to usage guidelines or restrictions to access the model or implementing safety filters.
    - Datasets that have been scraped from the Internet could pose safety risks. The authors should describe how they avoided releasing unsafe images.
    - We recognize that providing effective safeguards is challenging, and many papers do not require this, but we encourage authors to take this into account and make a best faith effort.

12. **Licenses for existing assets**

    Question: Are the creators or original owners of assets (e.g., code, data, models), used in the paper, properly credited and are the license and terms of use explicitly mentioned and properly respected?

    Answer: [Yes]

    Justification: We use an open-source dataset FractalDB, we cite the original paper and indicates the version we use in Section 4.1.

    Guidelines:

    - The answer NA means that the paper does not use existing assets.
    - The authors should cite the original paper that produced the code package or dataset.
    - The authors should state which version of the asset is used and, if possible, include a URL.
    - The name of the license (e.g., CC-BY 4.0) should be included for each asset.
    - For scraped data from a particular source (e.g., website), the copyright and terms of service of that source should be provided.
    - If assets are released, the license, copyright information, and terms of use in the package should be provided. For popular datasets, `paperswithcode.com/datasets` has curated licenses for some datasets. Their licensing guide can help determine the license of a dataset.

- For existing datasets that are re-packaged, both the original license and the license of the derived asset (if it has changed) should be provided.
- If this information is not available online, the authors are encouraged to reach out to the asset's creators.

13. **New Assets**

    Question: Are new assets introduced in the paper well documented and is the documentation provided alongside the assets?

    Answer: [Yes]

    Justification: We submit our assets in zip file and also put them on the anonymous github repository, we have included a README file with detailed descriptions.

    Guidelines:

    - The answer NA means that the paper does not release new assets.
    - Researchers should communicate the details of the dataset/code/model as part of their submissions via structured templates. This includes details about training, license, limitations, etc.
    - The paper should discuss whether and how consent was obtained from people whose asset is used.
    - At submission time, remember to anonymize your assets (if applicable). You can either create an anonymized URL or include an anonymized zip file.

14. **Crowdsourcing and Research with Human Subjects**

    Question: For crowdsourcing experiments and research with human subjects, does the paper include the full text of instructions given to participants and screenshots, if applicable, as well as details about compensation (if any)?

    Answer: [NA]

    Justification: This paper does not involve crowdsourcing nor research with human subjects.

    Guidelines:

    - The answer NA means that the paper does not involve crowdsourcing nor research with human subjects.
    - Including this information in the supplemental material is fine, but if the main contribution of the paper involves human subjects, then as much detail as possible should be included in the main paper.
    - According to the NeurIPS Code of Ethics, workers involved in data collection, curation, or other labor should be paid at least the minimum wage in the country of the data collector.

15. **Institutional Review Board (IRB) Approvals or Equivalent for Research with Human Subjects**

    Question: Does the paper describe potential risks incurred by study participants, whether such risks were disclosed to the subjects, and whether Institutional Review Board (IRB) approvals (or an equivalent approval/review based on the requirements of your country or institution) were obtained?

    Answer: [NA]

    Justification: This paper does not involve crowdsourcing nor research with human subjects.

    Guidelines:

    - The answer NA means that the paper does not involve crowdsourcing nor research with human subjects.
    - Depending on the country in which research is conducted, IRB approval (or equivalent) may be required for any human subjects research. If you obtained IRB approval, you should clearly state this in the paper.
    - We recognize that the procedures for this may vary significantly between institutions and locations, and we expect authors to adhere to the NeurIPS Code of Ethics and the guidelines for their institution.
    - For initial submissions, do not include any information that would break anonymity (if applicable), such as the institution conducting the review.